Catal Lett (2008) 120:179–183
DOI 10.1007/s10562-007-9303-6

CO Adsorption on FeO_x Nanoclusters Supported on HOPG—Effect of Oxide Formation on Catalytic Activity

E. Kadossov · S. Funk · Uwe Burghaus

Received: 7 September 2007 / Accepted: 5 October 2007 / Published online: 23 October 2007

Abstract CO adsorption on FeO_x clusters has been characterized by thermal desorption spectroscopy (TDS) and molecular beam scattering. Iron was vapor deposited and oxidized by annealing in O_2. The TDS curves consist initially of two peaks indicating formation of γ-Fe_2O_3/Fe_3O_4. Increasing the O_2 exposure results in one TDS peak and the dominance of α-Fe_2O_3.

Keywords Surface chemistry · Kinetics · Dynamics · Thermal desorption spectroscopy · Auger electron spectroscopy · Molecular beam scattering · Carbon monoxide · HOPG · Iron oxide clusters

1 Introduction

Nanometer-sized metal oxide clusters currently attract significant interest due to their high catalytic activity which may be related with unique properties of the metal/oxide interface [1–6]. Furthermore, iron oxide clusters and thin films are pertinent for a variety of applications including catalysis [7, 8], magnetic sensing [9, 10], data storage [11], spintronics, and biological systems [12]. In addition, iron oxide particles have been identified as a component of particulate matter in the plume of coal combustion plants which may have serious implications on human health [13]. Iron oxide clusters are complicated by the large number of different oxide phases (from FeO to Fe_2O_3 with oxidation states of +2 and +3 including mixed valency compounds) [7] and their complex morphology (e.g., the shell and core of nanoparticles may have different size-dependent structures exposing different surfaces) [14, 15]. Therefore, it appears pertinent to address how the oxidation state of small iron oxide clusters affects the catalytic activity towards adsorption of standard surface chemistry probe molecules such as CO.

According to scanning tunneling microscopy (STM) [16] data, Fe clusters occupy preferentially terrace edges, particularly after annealing (3 min at 800 K), on HOPG (highly oriented pyrolitic graphite) which has been chosen as a support in this study. The growth is characterized by a narrow particle size distribution centred at $\sim$6 nm for two monolayer (ML) Fe deposition. In most single crystal studies initially the formation of mixed Fe_2O_3 (maghemite)/Fe_3O_4 (magnetite) oxides has been reported [7, 17]. In a recent transmission electron microscopy investigation [14, 15] it has been shown that Fe nanoparticles with diameters below 8 nm fully oxidize and form a polycrystalline phase. For larger particles, a single crystalline Fe core is evident which is encapsulated by polycrystalline iron oxide nanoparticles; mixed Fe_2O_3/Fe_3O_4 oxides form. Although a wealth of kinetic studies have been conducted on clean HOPG (see e.g., Refs. 18–20) we are only aware of a few molecular beam scattering projects [21–25]. In addition, still rather few molecular beam scattering studies have been conducted on supported model catalysts [26–28]. We are not aware of CO thermal desorption spectroscopy (TDS) or molecular beam scattering projects on iron oxide clusters.

In this study we attempt to correlate qualitatively the oxidation state of iron oxide clusters with the catalytic activity for CO adsorption by means of kinetics (TDS) and dynamics (molecular beam scattering) measurements.

E. Kadossov · S. Funk · U. Burghaus (✉)
Department of Chemistry, Biochemistry, and Molecular Biology, North Dakota State University, 1231 Albrecht blv., Fargo, ND 58105, USA
e-mail: uwe.burghaus@ndsu.edu

2 Experimental Procedures

The measurements have been conducted by a home-built, triply differentially pumped molecular beam system [29]. The supersonic beam is attached to a scattering chamber which contains a shielded mass spectrometer for TDS [30] and adsorption probability measurements, an Auger electron spectrometer (AES), and a home-built metal evaporator. Iron (Goodfellow 99.95%) was vapor deposited on HOPG at room temperature with the vacuum chamber at a base pressure below 3×10^{-10} mbar. The equivalent Fe coverage has been estimated from AES and CO TDS measurements. The impact energy, E_i, of the CO molecules could be varied within 0.09–0.7 eV by using pure CO and seeding 3% CO in He, combined with a variation of the nozzle temperature within 300–650 K. For the TDS experiments CO also has been dosed on the sample with the molecular beam system, which keeps the background pressure while dosing the gas below 2×10^{-8} mbar. The reading of the thermocouple has been calibrated in situ by measuring the condensation temperature of alkanes.

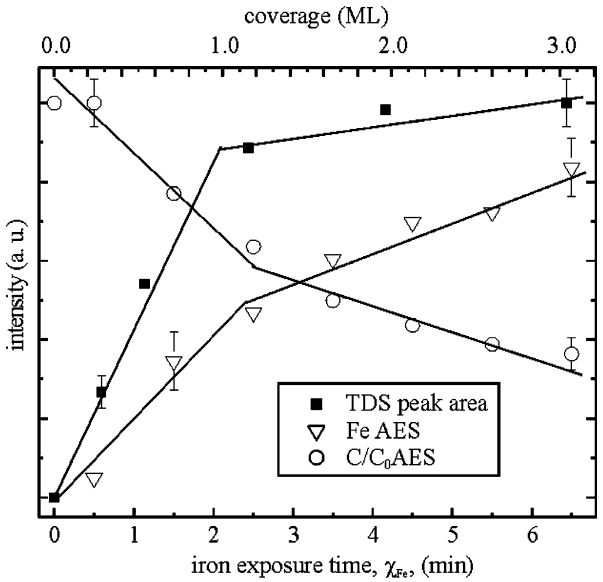

Fig. 1 Estimate of the Fe coverage by Auger electron spectroscopy (AES) and thermal desorption spectroscopy (TDS) (FeO_x with $x = 0.175$–0.275, deposition temperature of 300 K)

3 Data Presentation and Discussion

3.1 Estimate of Fe Coverage and Oxidation State

Figure 1 shows the Fe_{703} and C_{273} AES line intensities versus iron exposure time, χ_{Fe}, (open symbols). The intensities for all data shown are given in arbitrary units since only the shape of the curves is important. The AES intensities increase/decrease linearly with increasing χ_{Fe} with a change in the slope at about 2 min exposure time. This change in the slope likely indicates a transition from a two-dimensional (2D) cluster growth mode to the growth of thick 3D clusters. Therefore, we assign an exposure of 2 min to a nominal coverage of one ML (see upper scale in Fig. 1). Similar results have been obtained for metal-on-metal oxide systems [28] and Fe/TiO_2 (110) [5]. Consistent with this conclusion is the evolution of the CO TDS peak areas obtained as a function of χ_{Fe} (see solid symbols in Fig. 1).

Figure 2 depicts the effect of annealing the sample in oxygen ambient on the averaged stoichiometry of the iron oxide cluster ensemble. The Fe clusters have been oxidized at 500 K by backfilling the ultra-high vacuum (UHV) chamber with O_2 at 1×10^{-7}–1×10^{-6} mbar. The averaged stoichiometry (x in FeO_x) of the clusters has been estimated from the AES line intensities according to x = AES-O_{506}/AES-Fe_{703} and assuming sensitivity factors of 0.5 and 0.2 for oxygen and iron, respectively. At our best vacuum condition ($<3 \times 10^{-10}$ mbar) the averaged cluster stoichiometry amounts to $x = 0.18$ and increases to 1.5 while annealing the clusters in O_2 following a square root-like shape. The arrows in Fig. 2 depict the stoichiometries expected for the pure and perfectly crystalline oxide phases. Note that even crystalline $Fe_{1-\eta}O$ is commonly non-stochiometric. The initial averaged stoichiometry of $x = 0.18$ already indicates that metallic Fe clusters and mixed oxides coexist, consistent with earlier reports. Thus, the AES data do not reveal in a simple way the real stoichiometry of the clusters but they allow controlling the

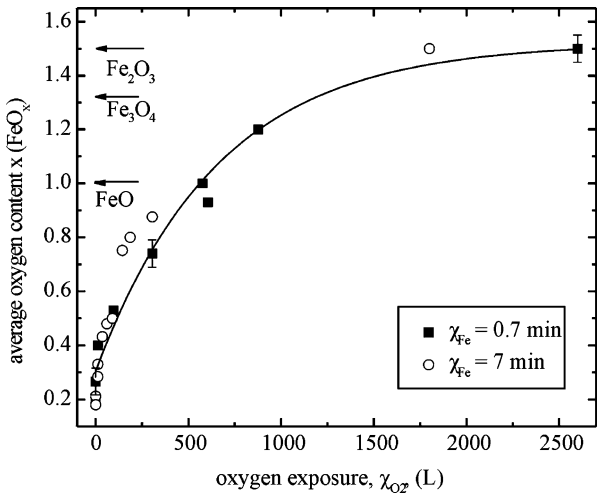

Fig. 2 Averaged stoichiometry (FeO_x) of the iron oxide cluster ensemble as a function of oxygen exposure for small and large amounts of Fe deposited on HOPG

measuring conditions such that a Fe cluster ensemble with a similar averaged oxidation state can be studied.

3.2 Adsorption Kinetics—Thermal Desorption Spectroscopy

Figure 3 depicts a set of CO TDS curves obtained for small (0.35 ML, χ_{Fe} = 0.7 min, upper panel) and large (3.5 ML, χ_{Fe} = 7 min, lower panel) amounts of iron as a function of the averaged stoichiometry. The oxygen exposure, χ_{O_2}, increases from top to bottom in each data set, cf. Fig. 2. The Fe clusters have been oxidized as described above and the sample has been saturated with CO (by means of the molecular beam system) at 100 K. Two TDS peaks labeled as α- and β-peaks are evident. The peak positions remains approximately constant at 150 K (α-peak) and at 250 K (β-peak). Assuming a pre-exponential factor of $10^{13}s^{-1}$ and first-order kinetics yields binding energies of 39 ± 2 and 65 ± 2 kJ/mol. At small O_2 exposures the β-peak dominates the TDS curves (Fig. 3a) but its intensity decreases with increasing χ_{O_2} (or x) with respect to the α-peak. Although no characterization of the sample's morphology is available, a kinetic structure–activity relationship (SAR) can be concluded since the different oxidation states of the Fe clusters should (despite possible differences in the electronic structure) correspond to different overall morphologies which are related (according to Fig. 3) to different binding energies of CO. Site blocking by water uptake from the UHV has been seen elsewhere [7], however, the desorption of H_2O was below the detection limit of our mass spectrometer. Therefore, we rule out site blocking effects with impurities as the reason for the quenching of the α-TDS peak with increasing oxygen exposure.

We assign the α-TDS peak to Fe^{3+} and the β-TDS peak to Fe^{2+} cation adsorption sites, forming initially an ensemble of Fe, γ-Fe_2O_3 and Fe_3O_4 clusters. These oxides are mixed valency oxides, in agreement with this TDS peak assignment. A perfect one-to-one intensity ratio of the α/β-TDS peaks cannot be expected for a mixed ensemble of clusters which clearly consists also of metallic Fe (initial stoichiometry x = 0.18). The mixing ratio (i.e., the stoichiometry, see Fig. 2) of the iron oxide clusters changes with oxygen exposures, since the intensity ratio of the α- and β-TDS peaks depends on χ_{O_2}. Therefore, at large oxygen exposures, where only the α-TDS peak has been detected, the ensemble of clusters is dominated by the formation of a more pure (in terms of the stoichiometry) α-Fe_2O_3-like oxide and a Fe valence of +3. A reversed assignment of the TDS peaks would require assuming the formation of FeO (at large annealing times in oxygen) which does not appear plausible since in this case the

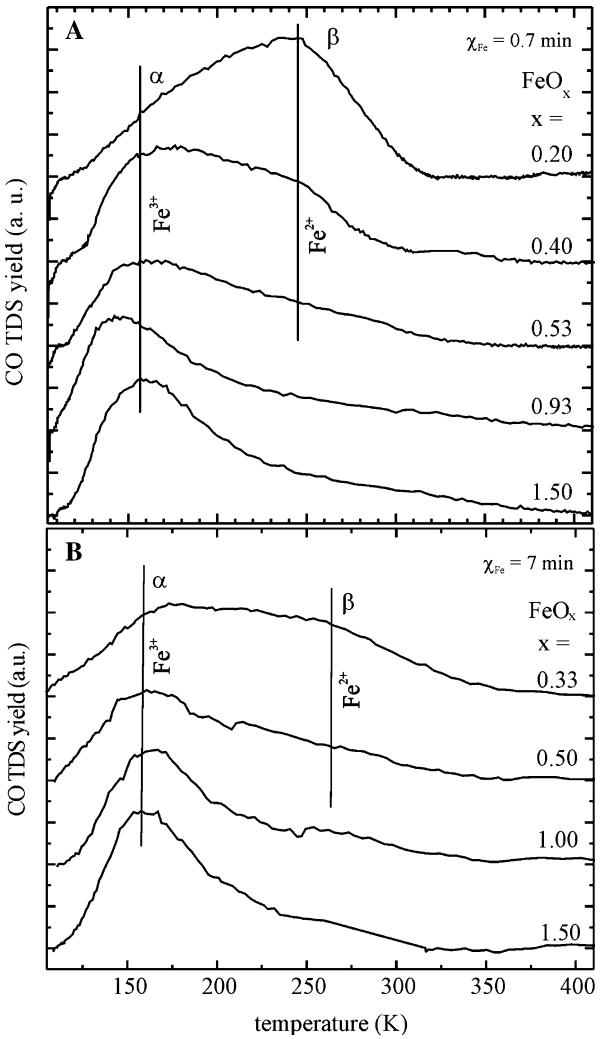

Fig. 3 TDS data for (**a**) small (χ_{Fe} = 0.7 min) and (**b**) large (χ_{Fe} = 7 min) amounts of Fe deposited on HOPG as a function of oxygen exposure (FeO_x stoichiometry). The samples have been annealed for 0–30 min at 10^{-7}–10^{-6} mbar at 500 K. Heating rate for TDS amounts to 1.3 K/s

oxygen content of the iron oxide clusters would decrease with increasing oxygen annealing time. CO adsorbed at metallic iron desorbs at much larger temperatures; TDS features at 700 K have been detected [31, 32].[1] The data suggest that polycrystalline Fe clusters form which are characterized by a mixture of different crystallographic orientations, as seen in recent electron microscopy studies [14, 15].

[1] Although we have seen CO desorption above 700 K, quantifying the amount of metallic Fe by CO TDS would be questionable with our setup since the entire sample holder is warming up at such large temperatures. Although a shielded mass spectrometer is used in this study, the contributions from the sample holder would still be difficult to quantify.

3.3 Adsorption Dynamics—Molecular Beam Scattering

In order to correlate the different (averaged) oxidation states with gas-surface energy transfer processes, CO adsorption probability measurements have been collected as a function of oxygen exposure (annealing time), χ_{O_2} (Fig. 4). On one hand, metal oxides have typically smaller initial adsorption probabilities, S_0, of small molecules than metal surfaces [29], i.e., S_0 would decrease with increasing x (stoichiometry). On the other hand, oxidized clusters should be larger than the corresponding metal clusters. According to the so-called capture zone model [33], this would lead to an increase in S_0 as x increases; thus, both effects can compensate each other, leading to a S_0 value independent of annealing time and x. In addition, cluster systems are strongly corrugated, which leads to efficient gas-surface energy transfer processes (i.e., small effects on S_0 with variations in the stoichiometry may be expected). However, it is difficulty to predict which of those effects will dominate, and so experimental data are required.

For the system considered here and at small Fe exposures, the initial adsorption probability, S_0, is independent of χ_{O_2}. Thus, the oxidation state of the Fe clusters does not affect the energy transfer processes within experimental accuracy. This may be expected for a largely corrugated (geometrically irregular) system, as described above; however, at large χ_{Fe}, a trend of decreasing S_0 is seen. At large χ_{Fe}, AES data confirms a decrease in the absolute amount of Fe (by $\sim$50%) while oxidizing the iron clusters, due to thermal desorption. (According to STM results [16] even for large Fe exposures, the clusters should still be small enough that AES data allow revealing the total amount of iron.) Thus, this decrease in S_0 is related with a particle size effect. Note that S_0 is systematically larger for larger amounts of deposited Fe. This result is typically observed for nanocluster systems [28] and can be explained by the capture zone model (CZM) [33]. Although the coverage of CO on the clean HOPG support is negligible at 100 K, CO molecules can still be trapped on the support long enough that the gas-phase species can diffuse to the clusters as large binding energy sites. The ratio of the surface residence time and diffusion lifetime defines the size of the capture zone; the larger the clusters, the larger the capture zone and the larger the S_0 value. Therefore, S_0 is systematically larger at large χ_{Fe} (Fig. 4). While oxidizing large amounts of Fe (see triangles in Fig. 4), the total amount of Fe decreases, which will reduce the cluster size; therefore, S_0 decreases slightly for χ_{Fe} = 7 min. More detailed beam scattering experiments have been conducted and will be discussed elsewhere. Briefly, S_0 decreases with impact energy consistent with molecular adsorption. S_0 decreases with temperature and at larger temperatures in agreement with CZM. The coverage dependence of the adsorption probability obeys shapes typical for precursor-mediated adsorption, as predicted by the CZM.

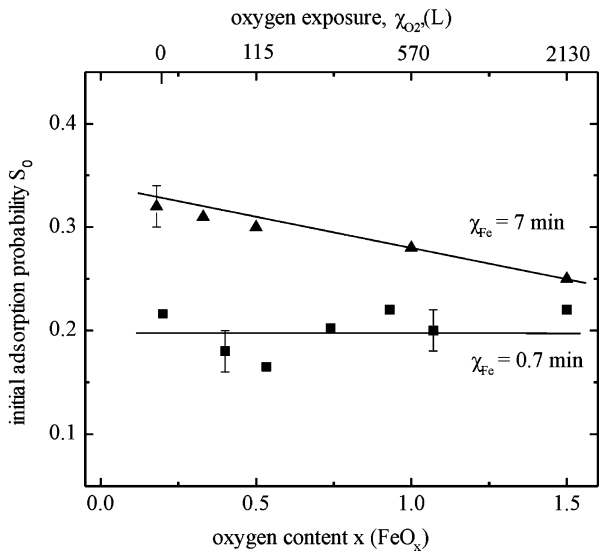

Fig. 4 Initial adsorption probability of CO for small and large amounts of Fe deposited on HOPG as a function of the averaged cluster stoichiometry (adsorption temperature of 105 K, E_i = 0.39 eV)

In summary, the following information has been collected for the complicated but technically important Fe-oxide cluster system supported on HOPG.

- Small Fe clusters readily oxidizes even at good ultra-high vacuum condition, i.e., a characterization of the oxidation state of small metal clusters appears important. (In some studies conducted at similar background pressures the oxidation state of Fe clusters has not been considered.)
- A kinetic structure–activity relationship (SAR) has been observed since two different CO TDS peaks are evident with an intensity ratio depending on the oxide stoichiometry and hence cluster morphology.
- The gas-surface energy transfer processes are little affected by the cluster stoichiometry as perhaps expected for a strongly corrugated/defected system.
- Kinetics (the binding energies) and dynamics (the adsorption probabilities) parameters have been quantified by TDS and molecular beam scattering.

Acknowledgments Financial support by the Department of Energy (DE-FG02-06ER46292; state grant, "coal combustion emission mechanism") is acknowledged. Assistance by Shannon Weidman (Fort-Berthold Tribal College, ND) in the initial stage of the project is noted.

References

1. White B, Yin M, Hall A, Le D, Stolbov S, Rahman T, Turro N, O'Brien S (2006) Nano Lett 6:2095
2. Wang LS, Wu H, Desai SR (1996) Phys Rev Lett 76:4853
3. Latham AH, Wilson MJ, Schiffer P, Williams MW (2006) J Am Chem Soc 128:12632
4. Schalow T, Brandt B, Starr DE, Laurin M, Shaikhutdinov DSK, Schauermann S, Libuda J, Freund HJ (2006) Angew Chem Int Ed Engl 45:3693
5. Mostefa-SBa H, Domenichini B, Bourgeois S (1999) Science 437:107
6. Roosendaal SJ, Vredenberg AM, Habraken FHPM (2000) Phys Rev Lett 84:3366
7. Weiss W, Ranke W (2002) Prog Surf Sci 70:1
8. Henderson MA, Jin T, White JM (1986) J Phys Chem 90:4607
9. Vescovo E, Kim HJ, Ablett JM, Chambers SA (2005) J Appl Phys 98:084507
10. Westphalen WA, Schmitte ST, Westerholt W, Zabel H (2005) J Appl Phys 97:073909
11. Bader SD (2002) Surf Sci 500:172
12. Cao D, Hu N (2006) Biophys Chem 121:209
13. Seames WS (2003) Fuel Process Technol 81:109
14. Wang CM, Baer DR, Amonette JE, Engelhard MH, Qiang Y, Antony J (2007) Nanotechnology 18:255603
15. Wang CM, Baer DR, Thomas LE, Amonette JE (2005) J Appl Phys 98:094308
16. Lopez-Salido I, Lim DC, Kim YD (2005) Surf Sci 588:6
17. Lemire C, Meyer R, Henrich VE, Shaikhutdinov Sh, Freund HJ (2004) Surf Sci 572:103
18. Lei RZ, Gellman AJ, Koel BE (2004) Surf Sci 554:125
19. Muller T, Flynn GW, Mathauser AT, Teplyakov AV (2003) Langmuir 19:2812
20. Kadossov E, Goering J, Burghaus U (2007) Surf Sci 601:3421
21. Nicholsen KT, Minton TK, Sibener SJ (2005) J Phy Chem B 109:8476
22. Kondo T, Mori D, Okada R, Sasaki M, Yamamoto S (2005) J Chem Phys 123:114712
23. Shimada T, Hasimoto R, Koide J, Kamimuta Y, Koma A (2000) Surf Sci 470:L52
24. Nagard MB, Andersson PU, Markovic N, Petterson JBC (1998) J Chem Phys 109:10339
25. Watanabe Y, Yamagucgi H, Masinokuchi M, Sawabe K, Maruyama S, Matsumoto Y, Shobatake K (2005) Chem Phys Lett 413:331
26. Henry CR (1998) Surf Sci Rep 31:235
27. Libuda J, Freund HJ (2005) Surf Sci Rep 57:157
28. Wang J, Burghaus U (2005) J Chem Phys 123:184716
29. Wang J, Burghaus U (2005) J Chem Phys 122:044705
30. Wang J, Hokkanen B, Burghaus U (2005) Surf Sci 577:158
31. Ganzmann I, Borgmann D, Wedler G (1992) Mol Phys 76:823
32. Erdoehelyi A, Anneser E, Bauer Th, Stephan K, Borgmann D, Wedler G (1990) Surf Sci 227:57
33. Rumpf F, Poppa H, Boudard M (1988) Langmuir 4:722